

# Quantum surface effects on quantum emitters coupled to surface plasmon polariton

Xin-Yue Liu,<sup>1,2</sup> Chun-Jie Yang<sup>3</sup>, and Jun-Hong An<sup>1,2,\*</sup>

<sup>1</sup>*School of Physical Science and Technology & Lanzhou Center for Theoretical Physics, Lanzhou University, Lanzhou 730000, China*

<sup>2</sup>*Key Laboratory of Quantum Theory and Applications of MoE & Key Laboratory of Theoretical Physics of Gansu Province, Lanzhou University, Lanzhou 730000, China*

<sup>3</sup>*School of Physics, Henan Normal University, Xinxiang 453007, China*

As an ideal platform to explore strong quantized light-matter interactions, surface plasmon polariton (SPP) has inspired many applications in quantum technologies. It was recently found that quantum surface effects (QSEs) of the metal, including nonlocal optical response, electron spill-out, and Landau damping, contribute additional loss sources to the SPP. Such a deteriorated loss of the SPP severely hinders its realization of long-distance quantum interconnect. Here, we investigate the non-Markovian dynamics of quantum emitters (QEs) coupled to a common SPP in the presence of the QSEs in a planar metal-dielectric nanostructure. A mechanism to overcome the dissipation of the QEs caused by the lossy SPP is discovered. We find that, as long as the QE-SPP bound states favored by the QSEs are formed, a dissipationless entanglement among the QEs is created. It leads to that the separated QEs are coherently correlated in a manner of the Rabi-like oscillation mediated by the SPP even experiencing the metal absorption. Our study on the QSEs refreshes our understanding of the light-matter interactions in the absorptive medium and paves the way for applying the SPP in quantum interconnect.

**Introduction.**—Confining light in scales below the diffraction limit, surface plasmon polariton (SPP) has attracted extensive attentions to explore strong light-matter interactions [1–7] and led to fascinating applications in quantum technologies [8–14]. Recent advances in nanotechnologies have enabled the precise fabrication of ultra-fine plasmonic nanostructures, in which the characteristic size of the system is reduced to the nanoscale [15–19]. It was surprisingly found that the experimental observations on the SPP in this scale exhibit considerable discrepancies from the theoretical predictions based on classical macroscopic electrodynamics under the local response approximation (LRA) [20–25]. Hence, it is paramount to rigorously understand the plasmon-mediated light-matter interactions in nanostructured systems.

Including nonlocal optical response, electron spill-out, and Landau damping [26–29], the quantum surface effects (QSEs) of the metal-dielectric interface become so strong that the plasmon-mediated light-matter interactions are dramatically modified when the system sizes reduce to the mean free path of electrons [30–33]. Microscopic treatment of plasmon excitations in a quantum mechanical setting can be performed by the time-dependent density functional theory [34]. However, it is typically restricted by its complexity and only applicable to small plasmonic systems. A nonclassical theory called Feibelman  $d$ -parameter method was established to treat the QSEs by introducing the induced surface charge and current, which are further incorporated into two surface response parameters via the modified mesoscopic boundary conditions for the Maxwell equations [30, 35–37]. The method bridges the gap between microscopic and macroscopic descriptions. It has revealed that the QSEs play significant roles in a broad range of phenomena of

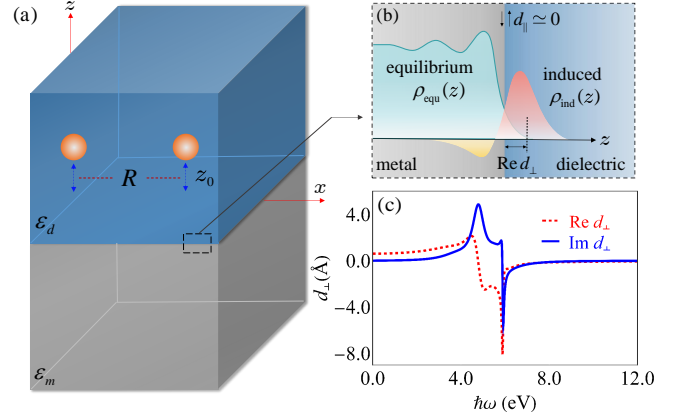


FIG. 1. (a) Schematic diagram of QEs separated by  $R$  and positioned at  $z_0$  above the metal.  $\epsilon_d$  is the permittivity of the dielectric and  $\epsilon_m$  is dielectric function of the metal. (b) A zoom-in view of the interface illustrates the equilibrium and induced electron densities and the Feibelman  $d$ -parameters. (c)  $d_\perp$  of sodium.  $d_\parallel$  vanishes due to the charge-neutrality.

the plasmon-mediated light-matter interactions, i.e., the enhancement of the Purcell factor [38, 39], the electron energy-loss spectroscopy [40], the dipole-forbidden transitions and the two-photon emission [37]. A striking feature of the QSEs is that they open an additional metal absorption to the SPP, which makes the lifetime of the SPP even shorter than the LRA predicted one [41, 42]. This severely restricts the applications of the SPP as a quantum bus in long-distance quantum interconnect devices [43, 44]. How to suppress the destructive influence of lossy SPPs on quantum emitters (QEs) is a key problem for applying the SPP in quantum technologies.

Here, we investigate the strong coupling between  $N$

QEs and the SPP in a planar metal-dielectric nanostructure in the presence of the QEs based on the macroscopic quantum electrodynamics (QED) and the Feibelman  $d$ -parameter methods. A mechanism to overcome the dissipation of QEs caused by the lossy SPP is uncovered. It is revealed that the dissipation of the QEs is suppressed and even a coherent quantum correlation among the QEs is persistently established whenever the QSE-favored bound states are formed in the energy spectrum of the total QE-SPP system. Solving the dissipation problem of the QEs induced by the lossy SPP, our finding enriches our understanding on light-matter interacting in absorptive medium and paves the way for utilizing the SPP in long-distance quantum devices.

*System.*— We study the interactions between  $N$  QEs and the SPP triggered by the radiation fields of the QEs on a planar metal-dielectric interface, see Fig. 1(a). The QEs separated in a distance  $R$  are embedded in the dielectric at a distance  $z_0$  above the interface and are modeled by two-level systems with a common frequency  $\omega_0$ . Their radiation field triggers three modes, i.e., the radiative mode in the dielectric, the non-radiative mode absorbed by the metal, and the SPP mode hybridized by the field and the electron-density wave on the metal-dielectric interface. The distinguished character of the SPP is that it confines the electromagnetic field (EMF) on the metal-dielectric interface beyond the diffraction limit. It makes the system an ideal platform to realize the strong light-matter interactions. To describe the quantum features in these interactions, a rigorous quantization scheme incorporating the three modes in inhomogeneous absorptive medium is needed. A macroscopic QED method based on the dyadic Green's tensor has been developed via describing the metal absorption to the EMF by a quantum noise, which guarantees the canonical commutation relations of the quantized field [45–52]. The quantized electric field reads

$$\hat{\mathbf{E}}(\mathbf{r}, \omega) = i\sqrt{\frac{\hbar\omega^4}{\pi\epsilon_0 c^4}} \int d^3\mathbf{r}' \sqrt{\text{Im}[\epsilon_m(\mathbf{r}, \mathbf{r}', \omega)]} \times \mathbf{G}(\mathbf{r}, \mathbf{r}', \omega) \cdot \hat{\mathbf{f}}(\mathbf{r}', \omega), \quad (1)$$

where  $\epsilon_0$  is the vacuum permittivity,  $\epsilon_m(\mathbf{r}, \mathbf{r}', \omega)$  is the nonlocal dielectric function of the metal,  $c$  is the speed of light, and  $\hat{\mathbf{f}}(\mathbf{r}, \omega)$  fulfilling  $[\hat{\mathbf{f}}(\mathbf{r}, \omega), \hat{\mathbf{f}}^\dagger(\mathbf{r}', \omega')] = \delta(\mathbf{r} - \mathbf{r}')\delta(\omega - \omega')$  is the annihilation operator of the field. The Green's tensor  $\mathbf{G}(\mathbf{r}, \mathbf{r}', \omega)$ , denoting the field in frequency  $\omega$  at  $\mathbf{r}$  triggered by a point source at  $\mathbf{r}'$ , is the solution of the Maxwell-Helmholtz equation  $[\nabla \times \nabla \times - \omega^2 c^{-2} \epsilon_m(\mathbf{r}, \mathbf{r}', \omega)]\mathbf{G}(\mathbf{r}, \mathbf{r}', \omega) = \mathbf{I}\delta(\mathbf{r} - \mathbf{r}')$ , where  $\mathbf{I}$  is the identity matrix. The scheme collects all the impacts of the metal-dielectric structure in the Green's tensor. The electric dipole interaction Hamiltonian of the total

system reads

$$\hat{H} = \sum_{i=1}^N \hbar\omega_0 \hat{\sigma}_i^\dagger \hat{\sigma}_i + \int_0^\infty d\omega \left\{ \int d^3\mathbf{r} \hbar\omega \hat{\mathbf{f}}^\dagger(\mathbf{r}, \omega) \cdot \hat{\mathbf{f}}(\mathbf{r}, \omega) - \sum_{i=1}^N [\boldsymbol{\mu}_i \cdot \hat{\mathbf{E}}(\mathbf{r}_i, \omega) \hat{\sigma}_i^\dagger + \text{H.c.}] \right\}, \quad (2)$$

where  $\hat{\sigma}_i = |g_i\rangle\langle e_i|$  is the transition operators from the excited state  $|e_i\rangle$  to the ground state  $|g_i\rangle$  and  $\boldsymbol{\mu}_i$  is the dipole moment of the  $i$ th QE.

The QSEs become strong and the classical treatment is insufficient when the QE-interface distance reduces to the mean free path of electrons [30–32]. It has three consequences. The first one is the spatial nonlocality of the dielectric function of the metal [26, 53, 54]. The second one is the spill-out of electrons from the metal [55, 56]. The last one is the surface Landau damping due to the decay of the plasma into the electron-hole pairs, which leads to an additional absorption source of the EMF in the metal [57–59]. The light-matter interactions modified by the QSEs can be effectively treated by introducing the Feibelman  $d$ -parameters  $d_\perp = \int_{-\infty}^\infty dz z \rho_{\text{ind}}(z) / \int_{-\infty}^\infty dz \rho_{\text{ind}}(z)$  and  $d_\parallel = \int_{-\infty}^\infty dz z \partial_z K_{\text{ind}}^x(z) / \int_{-\infty}^\infty dz \partial_z K_{\text{ind}}^x(z)$ , with the complex-valued  $\rho_{\text{ind}}(z)$  and  $K_{\text{ind}}^x(z)$  denoting the induced charge and current density near the interface by QSEs [36, 37]. The real parts of  $d_{\perp/\parallel}$  characterize the centroids of the induced charge and the normal derivative of the tangential current (see Fig. 1(b)), while the imaginary parts measure the surface-enabled damping [32, 60]. With the QSEs being encoded into  $d_{\perp/\parallel}$ , Feibelman's treatment permits us to localize the dielectric function in the bulk of the metal still as the classical Drude model  $\epsilon_m(\mathbf{r}, \mathbf{r}', \omega) \simeq \epsilon_m(\omega) = 1 - \omega_p^2 / [\omega(\omega + i\gamma_p)]$  [32, 61], where  $\omega_p$  is the bulk plasma frequency and  $\gamma_p$  is the damping factor of the EMF in the metal.

*Exact dynamics.*— It is easy to verify that the total excitation number  $\hat{\mathcal{N}} = \sum_i \hat{\sigma}_i^\dagger \hat{\sigma}_i + \int d^3\mathbf{r} \int d\omega \hat{\mathbf{f}}^\dagger(\mathbf{r}, \omega) \cdot \hat{\mathbf{f}}(\mathbf{r}, \omega)$  is conserved in the system. Thus, if only the first QE is excited and the EMF is in the vacuum state  $|\{0_{\mathbf{r}, \omega}\}\rangle$  initially, then the evolved state of the total system can be expanded as  $|\Psi(t)\rangle = [\sum_i a_i(t) \hat{\sigma}_i^\dagger + \int d^3\mathbf{r} \int d\omega b_{\mathbf{r}, \omega}(t) \hat{\mathbf{f}}^\dagger(\mathbf{r}, \omega)] |G; \{0_{\mathbf{r}, \omega}\}\rangle$ , where  $|G\rangle$  denotes that all the QEs are in the ground state and  $a_i(t)$  is the excited-state probability amplitude of the  $i$ th QE. According to the Schrödinger equation, we have

$$\dot{\mathbf{a}}(t) + i\omega_0 \mathbf{a}(t) + \int_0^t d\tau \int_0^\infty d\omega e^{-i\omega(t-\tau)} \mathbf{J}(\omega) \mathbf{a}(\tau) = 0, \quad (3)$$

where  $\mathbf{a}(t) = (a_1(t), \dots, a_N(t))^T$  is a column vector and  $\mathbf{J}(\omega)$  is a matrix of  $N$ -body spectral density with elements  $J_{ij}(\omega) = \omega^2 \boldsymbol{\mu}_i \cdot \text{Im}[\mathbf{G}(\mathbf{r}_i, \mathbf{r}_j, \omega)] \cdot \boldsymbol{\mu}_j^* / (\pi \hbar \epsilon_0 c^2)$  characterizing the correlations between the  $i$ th and  $j$ th QEs. Equation (3) indicates that indirect couplings among the QEs are induced by their direct interactions with the

common SPP. It is easy to verify  $J_{ij}(\omega) = J_{|i-j|}(\omega)$ . The convolution in Eq. (3) renders the dynamics non-Markovian, which is significant in quantum plasmonics due to the SPP enhanced light-matter interactions [44, 62, 63].

Choosing the dipole moments of the QEs being identical and normal to the interface, i.e.,  $\boldsymbol{\mu}_i = \mu \mathbf{e}_z$ , only  $G_{zz}(\mathbf{r}_i, \mathbf{r}_j, \omega)$  contributes to the dynamics. Solving the Maxwell-Helmholtz equation under the boundary condition modified by the QSEs, we obtain [64]

$$G_{zz}(\mathbf{r}_i, \mathbf{r}_j, \omega) = \int_0^\infty \frac{dk_s}{4\pi} \frac{i\mathcal{J}_0(k_s r_{\parallel}^{ij})}{k_d^2 k_{z_d/m} k_s^{-3}} (e^{ik_{z_d} z_{ij}^-} + r^p e^{ik_{z_d} z_{ij}^+}). \quad (4)$$

Here  $r_{\parallel}^{ij} = \sqrt{(x_i - x_j)^2 + (y_i - y_j)^2}$  and  $z_{ij}^\pm = z_i \pm z_j$ .  $\mathcal{J}_0$  is the zeroth-order Bessel function of the first kind.  $k_s$  and  $k_{z_d/m}$  satisfying  $k_s^2 + k_{z_d/m}^2 = k_{d/m}^2$ , with  $k_{d/m} = \sqrt{\varepsilon_{d/m}}\omega/c$  and  $\varepsilon_d$  being the permittivity of the dielectric, are the wave-vector components parallel and perpendicular to the dielectric-metal interface, respectively. The optical response of the interface to the EMF is collected in the reflection coefficient [30, 37, 64]

$$r^p = \frac{\varepsilon_m k_{z_d} - \varepsilon_d k_{z_m} + i(\varepsilon_m - \varepsilon_d)(k_s^2 d_{\perp} - k_{z_d} k_{z_m} d_{\parallel})}{\varepsilon_m k_{z_d} + \varepsilon_d k_{z_m} - i(\varepsilon_m - \varepsilon_d)(k_s^2 d_{\perp} + k_{z_d} k_{z_m} d_{\parallel})}. \quad (5)$$

In the limit of the large QE-interface distance,  $d_{\perp} = d_{\parallel} = 0$  and Eq. (5) naturally reduces to the LRA result [65, 66]. In the weak-coupling limit, the Markovian approximate solution of Eq. (3) is  $\mathbf{a}_{\text{MA}}(t) = \exp[-(\bar{\gamma}/2 + i\bar{\omega})t]\mathbf{a}(0)$ , where  $\bar{\gamma} = 2\pi\mathbf{J}(\omega_0)$  and  $\bar{\omega} = \omega_0\mathbf{I} + \mathcal{P} \int_0^\infty d\omega \mathbf{J}(\omega)/(\omega - \omega_0)$ , with  $\mathcal{P}$  being the Cauchy principal value. The positivity of  $\bar{\gamma}$  results in an exponential decay of  $|\mathbf{a}_{\text{MA}}(t)|$ , which means that all the QEs tend to their ground state in the long-time limit [67, 68]. It is harmful for applying the QEs in quantum technologies.

Although the non-Markovian solution of Eq. (3) is obtainable only via numerical calculation, its asymptotic form can be derived as follows. A Laplace transform converts Eq. (3) into  $\tilde{\mathbf{a}}(s) = [s + i\omega_0 + \int_0^\infty d\omega \frac{\mathbf{J}(\omega)}{s + i\omega}]^{-1}\mathbf{a}(0)$ . Then,  $\mathbf{a}(t)$  is the inverse Laplace transform of  $\tilde{\mathbf{a}}(s)$ , which needs finding its poles via

$$Y_j(\varpi) \equiv \omega_0 - \int_0^\infty d\omega \frac{A_j(\omega)}{\omega - \varpi} = \varpi, \quad (6)$$

where  $\varpi = is$  and  $A_j(\omega)$  is the  $j$ th eigenvalue of  $\mathbf{J}(\omega)$ . It is interesting to find that the roots  $\varpi$  multiplied by  $\hbar$  are the eigenenergies of Eq. (2) [64]. It indicates that dynamics of the QEs characterized by  $\mathbf{a}(t)$  is intrinsically determined by the features of the energy spectrum of Eq. (2). Because  $Y_j(\varpi)$  is a decreasing function in the region of  $\varpi < 0$ , Eq. (6) has a discrete root  $\varpi_j^b$  provided  $Y_j(0) < 0$ . The eigenstate of this discrete eigenenergy  $\hbar\varpi_j^b$  falling in the band-gap regime of the SPP is called a bound state, whose formation has profound impacts on the dynamics

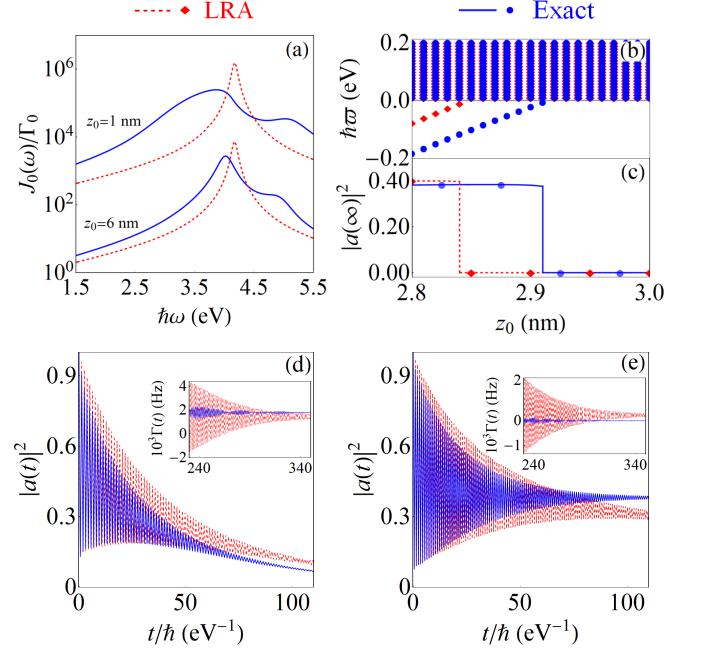


FIG. 2. (a) Ratio of  $J_0(\omega)$  and free-space spontaneous emission rate  $\Gamma_0 = \omega_0^3 \mu^2 / 3\pi \hbar \varepsilon_0 c^3$ , (b) energy spectrum (blue dots) by solving Eq. (6), and (c)  $|a(\infty)|^2$  (blue dots) by solving (3), with  $t/\hbar = 10^3 \text{ eV}^{-1}$ , in different  $z_0$ . The blue solid line in (c) is the analytic form  $L_0^2$ . Evolution of  $|a(t)|^2$  when (d)  $z_0 = 3.5 \text{ nm}$  and (e)  $2.9 \text{ nm}$ . The results under the LRA (red blocks or dashed lines) by setting  $d_{\perp} = 0$  are plotted for comparison. We use  $\hbar\omega_0 = 2.3 \text{ eV}$ ,  $\hbar\omega_p = 5.9 \text{ eV}$ , and  $\hbar\gamma_p = 0.1 \text{ eV}$ .

[44, 69]. In the region of  $\varpi > 0$ ,  $Y_j(\varpi)$  is ill defined and Eq. (6) has an infinite number of roots, which form a continuous energy band. Using the Cauchy's residue theorem, we obtain

$$\mathbf{a}(t) = \mathbf{Z}(t) + \int_0^\infty \frac{d\varpi}{2\pi} [\tilde{\mathbf{a}}(0^+ - i\varpi) - \tilde{\mathbf{a}}(0^- - i\varpi)] e^{-i\varpi t}, \quad (7)$$

where  $\mathbf{Z}(t) = \sum_{j=1}^M \text{Res}[\tilde{\mathbf{a}}(-i\varpi_j^b)] e^{-i\varpi_j^b t}$ , with  $\text{Res}[\cdot]$  denoting the residue contributed by the bound states, and  $M$  being the number of the bound states. The second term is from a branch cut formed by the continuous energy band and tends to zero in long-time limit due to the out-of-phase interference in continuously changing frequencies. Thus, if the bound state is absent, then  $\lim_{t \rightarrow \infty} \mathbf{a}(t) = 0$  characterizes a complete dissipation. It is consistent with the Markovian approximate [68, 70] and the previous results [37, 41]. If  $M$  bound states are formed, then  $\lim_{t \rightarrow \infty} \mathbf{a}(t) = \mathbf{Z}(t)$  implies a dissipation suppression. Being absent in the previous results, this result indicates that the non-Markovian effect in the strong-coupling regime plays a constructive role in suppressing the dissipation of the QEs caused by the lossy SPP.

*Results and discussion.*— It was previously found that the QSEs exert a reversible energy exchange between QEs

and SPP in the strong-coupling regime [37, 41]. However, the QEs exclusively dissipate to their ground states in the long-time limit. Our above analysis shows that the effects are also beneficial to suppress the QE dissipation and to preserve the coherent energy exchange among the QEs mediated by the SPP. To verify this, we choose sodium as the metal and obtain  $d_{\perp}$  by performing a numerical fitting to the data extracted from ab initio calculations [36, 37, 41], see Fig. 1(c). For this charge-neutral interface,  $d_{\parallel}$  vanishes [71].

First, we consider the case of  $N = 1$ . We can derive that a bound state with eigenenergy  $\hbar\varpi^b$  is present and  $Z(t) = L_0 e^{-i\varpi^b t}$ , with  $L_0 = [1 + \int d\omega J_0(\omega)/(\omega - \varpi^b)^2]^{-1}$ , when  $\omega_0 < \int_0^{\infty} d\omega J_0(\omega)/\omega$  [64]. Then the excited-state population has a long-time limit  $|a(\infty)|^2 = L_0^2$ . Figure 2(a) shows  $J_0(\omega)$  in different  $z_0$ . Under the LRA,  $J_0(\omega)$  shows one peak, which enables the SPP to be effectively described by a pseudo cavity mode with a Lorentzian spectrum. This method has been widely used in studying the strong QE-SPP coupling [70, 72]. In contrast to the LRA result, the QSEs cause a red shift and a broadening of the resonance plasmon peak on  $J_0(\omega)$ , which is attributed to the Landau damping [73], and a clear shoulder in the high-frequency regime, which relates to the electron spill-out [37]. These features make the Lorentzian fitting to  $J_0(\omega)$  in the pseudo-cavity method insufficient. The smaller the QE-surface distance, the stronger the QSEs. A common character between the exact and LRA  $J_0(\omega)$  is their enhancement over the spontaneous emission rate in free space in five orders of magnitude when  $z_0$  reaches the nanoscale. It is due to the sub-diffraction confinement to the EMF of the SPP. Manifesting a strong QE-SPP coupling, such an enhanced  $J_0(\omega)$  invalidates the Markovian approximation. To reveal the mechanism behind the non-Markovian dynamics, we plot the energy spectrum and  $|a(\infty)|^2$  in Figs. 2(b) and 2(c). Different from the complete vanishing in the Markovian approximation,  $|a(\infty)|^2$  matching with our analytic  $L_0^2$  exhibits an excited-state preservation once the bound state is formed. It is surprising that the QE can preserve its excited-state population even when it interacts with the EMF in such an absorptive medium. The governed mechanism is just the bound state, which is valid irrespective of whether the LRA is made or not. Compared with the LRA result, the QE-surface distance  $z_0$  in supporting the bound state in the exact result is enlarged. It indicates that the QSEs is helpful for forming the bound state and suppressing the dissipation of the QE. The rapid oscillations in the evolution of  $|a(t)|^2$  in Figs. 2(d) and 2(e) manifest the non-Markovian back-action effect. In the case of a large  $z_0$ , the bound state is absent for both the exact and LRA results and thus no qualitative difference is found between them, see Fig. 2(d). With decreasing  $z_0$ , the bound is still absent for the LRA one and the QE keeps decaying to the ground state, but it is present for the exact result,

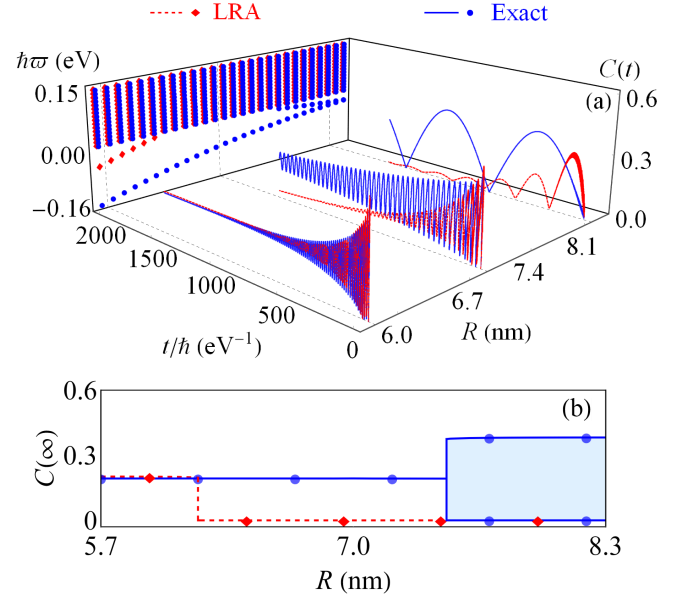


FIG. 3. (a) Energy spectrum and evolution of  $C(t)$  evaluated within LRA and exact calculations in different  $R$ . (b) Long-time values of  $C(t)$  obtained by dynamic evolution (solid and dashed lines) and bound-state analysis (circular and diamond points) in Eq. (8). We use  $z_0 = 2.9$  nm. Other parameters are the same as Fig. 2.

which results in a preserved excited-state population (see Fig. 2(e)). Thus, the QSEs signify their actions on the QE not only in the transient dynamics, but also in the steady state. This is further confirmed by that the decay rate  $\Gamma(t) \equiv -\text{Re}[\dot{a}(t)/a(t)]$  tends to a positive value in the absence of the bound state, meaning a complete dissipation, while tends to zero in the presence of the bound state, meaning a dissipation suppression, see the inset of Figs. 2(d) and 2(e).

Second, we consider  $N = 2$ . We obtain  $\mathbf{Z}(t) = \sum_{j=1}^M L_{01}^{(j)} (1, (-1)^{j+1})^T e^{-i\varpi_j^b t}$ , where  $L_{mn}^{(j)} = [1 + \int d\omega \frac{J_m(\omega) - (-1)^j J_n(\omega)}{(\omega - \varpi_j^b)^2}]^{-1/2}$  [64]. We study the entanglement of the QEs mediated by the SPP. The entanglement is measured by concurrence  $C = \max\{0, \sqrt{\lambda_1} - \sqrt{\lambda_2} - \sqrt{\lambda_3} - \sqrt{\lambda_4}\}$ , where  $\lambda_i$  are the eigenvalues of  $\rho(\hat{\sigma}_y \otimes \hat{\sigma}_y) \rho^*(\hat{\sigma}_y \otimes \hat{\sigma}_y)$  in decreasing order and  $\rho$  is the reduced density matrix of the QEs [74]. We can derive

$$\lim_{t \rightarrow \infty} C(t) = \begin{cases} 0, & M = 0 \\ 2L_{01}^{(1)2}, & M = 1 \\ 2|L_{01}^{(1)2} - L_{01}^{(2)2} + L(t)|, & M = 2, \end{cases} \quad (8)$$

where  $L(t) = 2iL_{01}^{(1)}L_{01}^{(2)} \sin[(\varpi_1^b - \varpi_2^b)t]$ . It is found that, if the bound state is absent, then no entanglement can be established in the long-time limit, which is consistent with the Markovian approximate result. If one bound state is present, then a stable entanglement is generated.



If two bound states are present, then a persistently oscillating entanglement is preserved, which signifies a lossless energy exchange between the QEs mediated by the SPP. These expectations are verified by the numerical calculation, see Figs. 3(a) and 3(b). We find from the energy spectrum in Fig. 3(a) that, in contrast to the LRA result that only one bound state is present, two bound states are present when the QE separation  $R$  is large in our exact result. The lossless energy exchange favored by the two bound states in the presence of the QSEs makes the two QEs coherently and permanently correlated in a manner of Rabi-like oscillation. This implies that our system could act as a quantum bus to remotely interconnect the QEs as quantum nodes [75, 76].

*Discussion and conclusion.*— Our scheme is realizable in the state-of-the-art experimental techniques. The detection of QSEs and its significant influence on plasmon-mediated light-matter interactions in nanostructured system has been realized [20, 24, 30, 77, 78]. The QEs could be quantum dot or J-aggregate, which can be selectively prepared in a single-excited state by optical or electrical drivings [79–81]. Modern manufacturing methods, including the nanopositioning techniques, the scanning QE methods, and the microfluidic flow control, enable the precise adjustment on positions of the QEs, which provides a strong support to achieve the strong QE-SPP coupling [82–84]. The bound state and its pivotal role in governing the non-Markovian dynamics of QEs have been observed in circuit QED [85, 86] and cold-atom systems [87, 88], which lays a firm foundation for the feasibility of implementation of our scheme in experiments.

In summary, we have investigated the QSEs on the QE-SPP interactions in a planar dielectric-metal nanostructure. We have discovered a mechanism to overcome the dissipation of the QEs caused by the lossy SPP in the presence of the additional metal absorption introduced by the surface-assisted nonlocal optical response, electron spill-out, and Landau damping. It is revealed that, with the formation of one and two bound states of the total QE-SPP system, the QEs, with the dissipation being efficiently suppressed, would be permanently correlated to a stable value and coherently correlated in a manner of Rabi-like oscillation in the long-time condition, respectively. The QSEs play a constructive role in establishing such a coherent correlation. The result enriches our understanding on plasmon-mediated light-matter interactions and is helpful for designing quantum interconnects and network by quantum plasmonics.

*Acknowledgments.*—This work was supported by the National Natural Science Foundation of China (Grants No. 12275109, No. 12074106, and No. 12247101), the Innovation Program for Quantum Science and Technology of China (Grant No. 2023ZD0300904), and the Natural Science Foundation of Henan Province (Grant No. 242300421165).

\* [anjhong@lzu.edu.cn](mailto:anjhong@lzu.edu.cn)

- [1] M. S. Tame, K. R. McEnery, Ş. K. Özdemir, J. Lee, S. A. Maier, and M. S. Kim, Quantum plasmonics, *Nat. Phys.* **9**, 329 (2013).
- [2] P. Törmä and W. L. Barnes, Strong coupling between surface plasmon polaritons and emitters: a review, *Reports on Progress in Physics* **78**, 013901 (2014).
- [3] S. Hu, J. Huang, R. Arul, A. Sánchez-Iglesias, Y. Xiong, L. M. Liz-Marzán, and J. J. Baumberg, Robust consistent single quantum dot strong coupling in plasmonic nanocavities, *Nature Communications* **15**, 6835 (2024).
- [4] N. S. Mueller, Y. Okamura, B. G. M. Vieira, S. Jürgensen, H. Lange, E. B. Barros, F. Schulz, and S. Reich, Deep strong light-matter coupling in plasmonic nanoparticle crystals, *Nature* **583**, 780 (2020).
- [5] J. Qin, Y.-H. Chen, Z. Zhang, Y. Zhang, R. J. Blaikie, B. Ding, and M. Qiu, Revealing strong plasmon-exciton coupling between nanogap resonators and two-dimensional semiconductors at ambient conditions, *Phys. Rev. Lett.* **124**, 063902 (2020).
- [6] Y. Niu, H. Xu, and H. Wei, Unified scattering and photoluminescence spectra for strong plasmon-exciton coupling, *Phys. Rev. Lett.* **128**, 167402 (2022).
- [7] L. Yang, X. Xie, J. Yang, M. Xue, S. Wu, S. Xiao, F. Song, J. Dang, S. Sun, Z. Zuo, J. Chen, Y. Huang, X. Zhou, K. Jin, C. Wang, and X. Xu, Strong light-matter interactions between gap plasmons and two-dimensional excitons under ambient conditions in a deterministic way, *Nano Lett.* **22**, 2177 (2022).
- [8] D. E. Chang, A. S. Sørensen, E. A. Demler, and M. D. Lukin, A single-photon transistor using nanoscale surface plasmons, *Nature Physics* **3**, 807 (2007).
- [9] R. Dhama, A. Panahpour, T. Pihlava, D. Ghindani, and H. Caglayan, All-optical switching based on plasmon-induced enhancement of index of refraction, *Nature Communications* **13**, 3114 (2022).
- [10] J. Ho, J. Tatebayashi, S. Sergent, C. F. Fong, Y. Ota, S. Iwamoto, and Y. Arakawa, A nanowire-based plasmonic quantum dot laser, *Nano Lett.* **16**, 2845 (2016).
- [11] C. Lee, B. Lawrie, R. Pooser, K.-G. Lee, C. Rockstuhl, and M. Tame, Quantum plasmonic sensors, *Chem. Rev.* **121**, 4743 (2021).
- [12] N. Zhou, Y. Yang, X. Guo, J. Gong, Z. Shi, Z. Yang, H. Wu, Y. Gao, N. Yao, W. Fang, P. Wang, and L. Tong, Strong mode coupling-enabled hybrid photon-plasmon laser with a microfiber-coupled nanorod, *Sci. Adv.* **8**, eabn2026 (2022).
- [13] N. Kongsuwan, X. Xiong, P. Bai, J.-B. You, C. E. Png, L. Wu, and O. Hess, Quantum plasmonic immunoassay sensing, *Nano Lett.* **19**, 5853 (2019).
- [14] X. Gao, B. Jiang, A. E. Llacsahuanga Allica, K. Shen, M. A. Sadi, A. B. Solanki, P. Ju, Z. Xu, P. Upadhyaya, Y. P. Chen, S. A. Bhawe, and T. Li, High-contrast plasmonic-enhanced shallow spin defects in hexagonal boron nitride for quantum sensing, *Nano Lett.* **21**, 7708 (2021).
- [15] J. J. Baumberg, J. Aizpurua, M. H. Mikkelsen, and D. R. Smith, Extreme nanophotonics from ultrathin metallic gaps, *Nat. Mater.* **18**, 668 (2019).
- [16] C. Ciraci, R. T. Hill, J. J. Mock, Y. Urzhumov, A. I. Fernández-Domínguez, S. A. Maier, J. B. Pendry,

- A. Chilkoti, and D. R. Smith, Probing the ultimate limits of plasmon enhancement, *Science* **337**, 1072 (2012).
- [17] J. A. Scholl, A. L. Koh, and J. A. Dionne, Quantum plasmon resonances of individual metallic nanoparticles, *Nature* **483**, 421 (2012).
- [18] R. Chikkaraddy, B. de Nijs, F. Benz, S. J. Barrow, O. A. Scherman, E. Rosta, A. Demetriadou, P. Fox, O. Hess, and J. J. Baumberg, Single-molecule strong coupling at room temperature in plasmonic nanocavities, *Nature* **535**, 127 (2016).
- [19] D. O. Sigle, J. Mertens, L. O. Herrmann, R. W. Bowman, S. Ithurria, B. Dubertret, Y. Shi, H. Y. Yang, C. Tserkezis, J. Aizpurua, and J. J. Baumberg, Monitoring morphological changes in 2D monolayer semiconductors using atom-thick plasmonic nanocavities, *ACS Nano* **9**, 825 (2015).
- [20] S. Boroviks, Z.-H. Lin, V. A. Zenin, M. Ziegler, A. Delith, P. A. D. Gonçalves, C. Wolff, S. I. Bozhevolnyi, J.-S. Huang, and N. A. Mortensen, Extremely confined gap plasmon modes: when nonlocality matters, *Nat. Commun.* **13**, 3105 (2022).
- [21] M. Khalid and C. Ciraci, Enhancing second-harmonic generation with electron spill-out at metallic surfaces, *Commun. Phys.* **3**, 214 (2020).
- [22] C. Tao, Y. Zhong, and H. Liu, Quasinormal mode expansion theory for mesoscale plasmonic nanoresonators: An analytical treatment of nonclassical electromagnetic boundary condition, *Phys. Rev. Lett.* **129**, 197401 (2022).
- [23] C. Ciraci, R. Jurga, M. Khalid, and F. D. Sala, Plasmonic quantum effects on single-emitter strong coupling, *Nanophotonics* **8**, 1821 (2019).
- [24] K. J. Savage, M. M. Hawkeye, R. Esteban, A. G. Borisov, J. Aizpurua, and J. J. Baumberg, Revealing the quantum regime in tunnelling plasmonics, *Nature* **491**, 574 (2012).
- [25] P. A. D. Gonçalves, T. Christensen, N. M. R. Peres, A.-P. Jauho, I. Epstein, F. H. L. Koppens, M. Soljačić, and N. A. Mortensen, Quantum surface-response of metals revealed by acoustic graphene plasmons, *Nat. Commun.* **12**, 3271 (2021).
- [26] S. Raza, S. Kadkhodazadeh, T. Christensen, M. Di Vece, M. Wubs, N. A. Mortensen, and N. Stenger, Multipole plasmons and their disappearance in few-nanometre silver nanoparticles, *Nat. Commun.* **6**, 8788 (2015).
- [27] D. Jin, Q. Hu, D. Neuhauser, F. von Cube, Y. Yang, R. Sachan, T. S. Luk, D. C. Bell, and N. X. Fang, Quantum-spillover-enhanced surface-plasmonic absorption at the interface of silver and high-index dielectrics, *Phys. Rev. Lett.* **115**, 193901 (2015).
- [28] S. Raza, S. I. Bozhevolnyi, M. Wubs, and N. A. Mortensen, Nonlocal optical response in metallic nanostructures, *J. Phys.: Condens. Matter* **27**, 183204 (2015).
- [29] H. M. Baghrmian, F. Della Sala, and C. Ciraci, Laplacian-level quantum hydrodynamic theory for plasmonics, *Phys. Rev. X* **11**, 011049 (2021).
- [30] Y. Yang, D. Zhu, W. Yan, A. Agarwal, M. Zheng, J. D. Joannopoulos, P. Lalanne, T. Christensen, K. K. Berggren, and M. Soljačić, A general theoretical and experimental framework for nanoscale electromagnetism, *Nature* **576**, 248 (2019).
- [31] S. Raza, N. Stenger, S. Kadkhodazadeh, S. V. Fischer, N. Kotesha, A.-P. Jauho, A. Burrows, M. Wubs, and N. A. Mortensen, Blueshift of the surface plasmon resonance in silver nanoparticles studied with EELS, *Nanophotonics* **2**, 131 (2013).
- [32] P. E. Stamatopoulou and C. Tserkezis, Finite-size and quantum effects in plasmonics: manifestations and theoretical modelling [invited], *Opt. Mater. Express* **12**, 1869 (2022).
- [33] W. Zhu, R. Esteban, A. G. Borisov, J. J. Baumberg, P. Nordlander, H. J. Lezec, J. Aizpurua, and K. B. Crozier, Quantum mechanical effects in plasmonic structures with subnanometre gaps, *Nat. Commun.* **7**, 11495 (2016).
- [34] M. Marques and E. Gross, Time-dependent density functional theory, *Annu. Rev. Phys. Chem.* **55**, 427 (2004).
- [35] P. J. Feibelman, Surface electromagnetic fields, *Prog. Surf. Sci.* **12**, 287 (1982).
- [36] T. Christensen, W. Yan, A.-P. Jauho, M. Soljačić, and N. A. Mortensen, Quantum corrections in nanoplasmonics: Shape, scale, and material, *Phys. Rev. Lett.* **118**, 157402 (2017).
- [37] P. A. D. Gonçalves, T. Christensen, N. Rivera, A.-P. Jauho, N. A. Mortensen, and M. Soljačić, Plasmon-emitter interactions at the nanoscale, *Nat. Commun.* **11**, 366 (2020).
- [38] Q. Zhou, P. Zhang, and X.-W. Chen, Quasinormal mode theory for nanoscale electromagnetism informed by quantum surface response, *Phys. Rev. B* **105**, 125419 (2022).
- [39] M. H. Eriksen, C. Tserkezis, N. A. Mortensen, and J. D. Cox, Nonlocal effects in plasmon-emitter interactions, *Nanophotonics* **13**, 2741 (2024).
- [40] P. Gonçalves and F. J. García de Abajo, Interrogating quantum nonlocal effects in nanoplasmonics through electron-beam spectroscopy, *Nano Letters* **23**, 4242 (2023).
- [41] V. Karanikolas, I. Thanopoulos, J. D. Cox, T. Kuroda, J.-i. Inoue, N. A. Mortensen, E. Paspalakis, and C. Tserkezis, Quantum surface effects in strong coupling dynamics, *Phys. Rev. B* **104**, L201405 (2021).
- [42] C. Tserkezis, N. A. Mortensen, and M. Wubs, How non-local damping reduces plasmon-enhanced fluorescence in ultranarrow gaps, *Phys. Rev. B* **96**, 085413 (2017).
- [43] D. Awschalom, K. K. Berggren, H. Bernien, S. Bhawe, L. D. Carr, P. Davids, S. E. Economou, D. Englund, A. Faraon, M. Fejer, S. Guha, M. V. Gustafsson, E. Hu, L. Jiang, J. Kim, B. Korzh, P. Kumar, P. G. Kwiat, M. Lončar, M. D. Lukin, D. A. Miller, C. Monroe, S. W. Nam, P. Narang, J. S. Orcutt, M. G. Raymer, A. H. Safavi-Naeini, M. Spiropulu, K. Srinivasan, S. Sun, J. Vučković, E. Waks, R. Walsworth, A. M. Weiner, and Z. Zhang, Development of quantum interconnects (QuICs) for next-generation information technologies, *PRX Quantum* **2**, 017002 (2021).
- [44] C.-J. Yang, X.-Y. Liu, S.-Q. Xia, S.-Y. Bai, and J.-H. An, Non-Markovian quantum interconnect formed by a surface plasmon polariton waveguide, *Phys. Rev. A* **109**, 033518 (2024).
- [45] T. Gruner and D.-G. Welsch, Green-function approach to the radiation-field quantization for homogeneous and inhomogeneous Kramers-Kronig dielectrics, *Phys. Rev. A* **53**, 1818 (1996).
- [46] N. Rivera and I. Kaminer, Light-matter interactions with photonic quasiparticles, *Nat. Rev. Phys.* **2**, 538 (2020).
- [47] S. Franke, J. Ren, M. Richter, A. Knorr, and S. Hughes, Fermi's golden rule for spontaneous emission in absorptive and amplifying media, *Phys. Rev. Lett.* **127**, 013602 (2021).

- [48] W. Nie, M. Antezza, Y.-x. Liu, and F. Nori, Dissipative topological phase transition with strong system-environment coupling, *Phys. Rev. Lett.* **127**, 250402 (2021).
- [49] S. Franke, S. Hughes, M. K. Dezfouli, P. T. Kristensen, K. Busch, A. Knorr, and M. Richter, Quantization of quasinormal modes for open cavities and plasmonic cavity quantum electrodynamics, *Phys. Rev. Lett.* **122**, 213901 (2019).
- [50] M. Richter and S. Hughes, Enhanced TEMPO algorithm for quantum path integrals with off-diagonal system-bath coupling: Applications to photonic quantum networks, *Phys. Rev. Lett.* **128**, 167403 (2022).
- [51] J. E. Vázquez-Lozano and I. Liberal, Incandescent temporal metamaterials, *Nat. Commun.* **14**, 4606 (2023).
- [52] J. Feist, A. I. Fernández-Domínguez, and F. J. García-Vidal, Macroscopic QED for quantum nanophotonics: emitter-centered modes as a minimal basis for multiemitter problems, *Nanophotonics* **10**, 477 (2021).
- [53] E. J. C. Dias, D. A. Iranzo, P. A. D. Gonçalves, Y. Hajati, Y. V. Bludov, A.-P. Jauho, N. A. Mortensen, F. H. L. Koppens, and N. M. R. Peres, Probing nonlocal effects in metals with graphene plasmons, *Phys. Rev. B* **97**, 245405 (2018).
- [54] C. Tserkezis, N. Stefanou, M. Wubs, and N. A. Mortensen, Molecular fluorescence enhancement in plasmonic environments: exploring the role of nonlocal effects, *Nanoscale* **8**, 17532 (2016).
- [55] G. Toscano, J. Straubel, A. Kwiatkowski, C. Rockstuhl, F. Evers, H. Xu, N. Asger Mortensen, and M. Wubs, Resonance shifts and spill-out effects in self-consistent hydrodynamic nanoplasmonics, *Nat. Commun.* **6**, 7132 (2015).
- [56] K. Ding and C. T. Chan, Plasmonic modes of polygonal rods calculated using a quantum hydrodynamics method, *Phys. Rev. B* **96**, 125134 (2017).
- [57] J. B. Khurgin, Ultimate limit of field confinement by surface plasmon polaritons, *Faraday Discuss.* **178**, 109 (2015).
- [58] T. V. Shahbazyan, Landau damping of surface plasmons in metal nanostructures, *Phys. Rev. B* **94**, 235431 (2016).
- [59] X. Li, D. Xiao, and Z. Zhang, Landau damping of quantum plasmons in metal nanostructures, *New Journal of Physics* **15**, 023011 (2013).
- [60] N. A. Mortensen, S. Raza, M. Wubs, T. Søndergaard, and S. I. Bozhevolnyi, A generalized non-local optical response theory for plasmonic nanostructures, *Nat. Commun.* **5**, 3809 (2014).
- [61] J. Kong, A. J. Shvonski, and K. Kempa, Nonlocal response with local optics, *Phys. Rev. B* **97**, 165423 (2018).
- [62] J. del Pino, F. A. Y. N. Schröder, A. W. Chin, J. Feist, and F. J. Garcia-Vidal, Tensor network simulation of non-Markovian dynamics in organic polaritons, *Phys. Rev. Lett.* **121**, 227401 (2018).
- [63] T. V. Shahbazyan, Non-Markovian effects for hybrid plasmonic systems in the strong coupling regime, *Phys. Rev. B* **105**, 245411 (2022).
- [64] See the Supplemental Material for a demonstration of Feibelman  $d$ -parameter method and a detailed derivation of the reflection coefficient, the Green's function of the metallic nanowire, the energy spectrum of the QE-SPP system, and the steady-state solutions.
- [65] L. Novotny and B. Hecht, *Principles of Nano-optics* (Cambridge University Press, Cambridge, UK, 2012).
- [66] C.-t. Tai, *Dyadic Green functions in electromagnetic theory*, 2nd ed. (New York (N.Y.) : IEEE press, 1994).
- [67] D. Dzsotjan, A. S. Sørensen, and M. Fleischhauer, Quantum emitters coupled to surface plasmons of a nanowire: A Green's function approach, *Phys. Rev. B* **82**, 075427 (2010).
- [68] A. Gonzalez-Tudela, F. J. Rodríguez, L. Quiroga, and C. Tejedor, Dissipative dynamics of a solid-state qubit coupled to surface plasmons: From non-Markov to Markov regimes, *Phys. Rev. B* **82**, 115334 (2010).
- [69] C.-J. Yang, J.-H. An, and H.-Q. Lin, Signatures of quantized coupling between quantum emitters and localized surface plasmons, *Phys. Rev. Res.* **1**, 023027 (2019).
- [70] A. González-Tudela, P. A. Huidobro, L. Martín-Moreno, C. Tejedor, and F. J. García-Vidal, Reversible dynamics of single quantum emitters near metal-dielectric interfaces, *Phys. Rev. B* **89**, 041402 (2014).
- [71] A. Liebsch, *Electronic excitations at metal surfaces* (Springer Science, New York, 1997).
- [72] F.-Z. Ji and J.-H. An, Kerr nonlinearity induced strong spin-magnon coupling, *Phys. Rev. B* **108**, L180409 (2023).
- [73] J. Khurgin, W.-Y. Tsai, D. P. Tsai, and G. Sun, Landau damping and limit to field confinement and enhancement in plasmonic dimers, *ACS Photonics* **4**, 2871 (2017).
- [74] W. K. Wootters, Entanglement of formation of an arbitrary state of two qubits, *Phys. Rev. Lett.* **80**, 2245 (1998).
- [75] Z.-K. Zhou, J. Liu, Y. Bao, L. Wu, C. E. Png, X.-H. Wang, and C.-W. Qiu, Quantum plasmonics get applied, *Prog. Quantum Electron.* **65**, 1 (2019).
- [76] S. I. Bogdanov, A. Boltasseva, and V. M. Shalae, Overcoming quantum decoherence with plasmonics, *Science* **364**, 532 (2019).
- [77] S. A. Maier and H. A. Atwater, Plasmonics: Localization and guiding of electromagnetic energy in metal/dielectric structures, *J. Appl. Phys.* **98**, 011101 (2005).
- [78] L. Zurak, C. Wolff, J. Meier, R. Kullo, N. A. Mortensen, B. Hecht, and T. Feichtner, Modulation of surface response in a single plasmonic nanoresonator, *Sci. Adv.* **10**, eadn5227 (2024).
- [79] S. Stobbe, J. Johansen, P. T. Kristensen, J. M. Hvam, and P. Lodahl, Frequency dependence of the radiative decay rate of excitons in self-assembled quantum dots: Experiment and theory, *Phys. Rev. B* **80**, 155307 (2009).
- [80] H. Fidder, J. Knoester, and D. A. Wiersma, Superradiant emission and optical dephasing in J-aggregates, *Chemical Physics Letters* **171**, 529 (1990).
- [81] P. Rai, N. Hartmann, J. Berthelot, J. Arocas, G. Colas des Francs, A. Hartschuh, and A. Bouhelier, Electrical excitation of surface plasmons by an individual carbon nanotube transistor, *Phys. Rev. Lett.* **111**, 026804 (2013).
- [82] H. Memmi, O. Benson, S. Sadofev, and S. Kalusniak, Strong coupling between surface plasmon polaritons and molecular vibrations, *Phys. Rev. Lett.* **118**, 126802 (2017).
- [83] J. Bellessa, C. Bonnard, J. C. Plenet, and J. Mugnier, Strong coupling between surface plasmons and excitons in an organic semiconductor, *Phys. Rev. Lett.* **93**, 036404 (2004).
- [84] T. K. Hakala, J. J. Toppari, A. Kuzyk, M. Pettersson, H. Tikkani, H. Kunttu, and P. Törmä, Vacuum Rabi splitting and strong-coupling dynamics for surface-

- plasmon polaritons and Rhodamine 6G molecules, *Phys. Rev. Lett.* **103**, 053602 (2009).
- [85] Y. Liu and A. A. Houck, Quantum electrodynamics near a photonic bandgap, *Nat. Phys.* **13**, 48 (2017).
  - [86] N. M. Sundaesan, R. Lundgren, G. Zhu, A. V. Gorshkov, and A. A. Houck, Interacting qubit-photon bound states with superconducting circuits, *Phys. Rev. X* **9**, 011021 (2019).
  - [87] L. Krinner, M. Stewart, A. Pazmiño, J. Kwon, and D. Schneble, Spontaneous emission of matter waves from a tunable open quantum system, *Nature* **559**, 589 (2018).
  - [88] J. Kwon, Y. Kim, A. Lanuza, and D. Schneble, Formation of matter-wave polaritons in an optical lattice, *Nat. Phys.* **18**, 657 (2022).



# Supplemental material for “Quantum surface effects on quantum emitters coupled to surface plasmon polariton”

Xin-Yue Liu,<sup>1,2</sup> Chun-Jie Yang<sup>1,3</sup> and Jun-Hong An<sup>1,2,\*</sup>

<sup>1</sup>*School of Physical Science and Technology & Lanzhou Center for Theoretical Physics, Lanzhou University, Lanzhou 730000, China*

<sup>2</sup>*Key Laboratory of Quantum Theory and Applications of MoE & Key Laboratory of Theoretical Physics of Gansu Province, Lanzhou University, Lanzhou 730000, China*

<sup>3</sup>*School of Physics, Henan Normal University, Xinxiang 453007, China*

## I. FEIBELMAN $d$ -PARAMETER METHOD

The macroscopic electromagnetic boundary conditions neglect the intrinsic electronic length scale associated with interfaces. This omission leads to significant discrepancies between classical predictions and experimental observations in systems with deeply nanoscale feature-sizes, typically evident below 10 nm to 20 nm. The Feibelman method reintroduces the electronic length scales by amending the classical boundary conditions with a set of mesoscopic complex surface response functions. They enable a leading-order-accurate incorporation of the quantum surface effects including nonlocal response, electron spill-out, and surface-enabled Landau damping.

The lowest-order nonclassical corrections to the macroscopic electromagnetic results is realized by introducing the scattering coefficients of the electromagnetic field (EMF) on the metal-dielectric interface in the non-retarded regime [1, 2]. For this purpose, we consider that the metal and the dielectric have a planar interface at  $z = 0$ . When an EMF with a potential  $\phi_{\text{ext}}(\mathbf{r}) = e^{ikx+kz}$  impinges from the dielectric region ( $z > 0$ ) on the interface, a quantum charge density  $\rho_{\text{ind}}(\mathbf{r}) = \rho_{\text{ind}}(z)e^{ikx}$  is induced on the interface. An induced potential  $\phi_{\text{ind}}(\mathbf{r}) = \phi_{\text{ind}}(z)e^{ikx}$  generated by  $\rho_{\text{ind}}(z)$  is determined by the Coulomb's law as

$$\phi_{\text{ind}}(z) = \frac{1}{2\varepsilon_0 k} \int_{z_1}^{z_2} e^{-k|z-z'|} \rho_{\text{ind}}(z') dz', \quad (\text{S1})$$

where  $z_1 (< 0)$  and  $z_2 (> 0)$  are the positions far from the interface where  $\rho_{\text{ind}}(z)$  vanishes. Because the charge densities are sharply peaked near the interface, the asymptotic behavior of  $\phi_{\text{ind}}(z)$  beyond  $z_1$  and  $z_2$  can be obtained by expanding it around  $kz' = 0$ . Introducing a multipole expansion, we have

$$\phi_{\text{ind}}(z) = \frac{e^{-k|z|}}{2\varepsilon_0 k} \sigma \{1 + \text{sgn}(z)kd_{\perp} + O[(kz')^2]\}, \quad (\text{S2})$$

where  $\sigma = \int_{z_1}^{z_2} \rho_{\text{ind}}(z) dz$  and

$$d_{\perp} = \frac{1}{\sigma} \int_{z_1}^{z_2} z \rho_{\text{ind}}(z) dz \quad (\text{S3})$$

characterizes the position of the centroid of the induced surface charge density.

In order to obtain the optical scattering coefficients with non-classical corrections, we define an auxiliary potential  $\phi^{\infty}(z)$ , which agrees with the actual total potential  $\phi_{\text{ext}}(z) + \phi_{\text{ind}}(z)$  in the far-field asymptotic regions  $|z| \geq |z_{1/2}|$

$$\phi^{\infty}(z) = \begin{cases} e^{kz} + r^{\text{nr}} e^{-kz}, & z > 0 \\ t^{\text{nr}} e^{kz}, & z < 0 \end{cases}. \quad (\text{S4})$$

Here,  $r^{\text{nr}}$  and  $t^{\text{nr}}$  are the reflection and transmission coefficients in the non-retarded region. According to Eq. (S2), we obtain  $r^{\text{nr}} = \frac{1}{2\varepsilon_0 k} \sigma(1 + kd_{\perp})$  and  $t^{\text{nr}} = 1 + \frac{1}{2\varepsilon_0 k} \sigma(1 - kd_{\perp})$ . The continuity condition of  $\phi^{\infty}(z)$  and its derivative at  $z = 0$  results in

$$(1 - t^{\text{nr}})(1 + kd_{\perp}) + r^{\text{nr}}(1 - kd_{\perp}) = 0, \quad (\text{S5})$$

which is the first effective boundary condition.

A current  $\mathbf{K}_{\text{ind}}(\mathbf{r})$  is also induced by the EMF near the interface. Its impact on the scattering coefficients is viewed as the second effective boundary condition. To obtain it, a set of auxiliary classical charge and current densities, i.e.,  $\rho^{\infty}(\mathbf{r})$  and  $\mathbf{K}^{\infty}(\mathbf{r})$ , interrelated by the continuity equation  $\nabla \cdot \mathbf{K}^{\infty}(\mathbf{r}) - i\omega\rho^{\infty}(\mathbf{r}) = 0$  has to be introduced. Here,  $\mathbf{K}^{\infty}(\mathbf{r}) = \mathbf{K}^{\infty}(z)e^{ikx}$  approaches  $\mathbf{K}_{\text{ind}}(\mathbf{r})$  in the asymptotic regions  $|z| \geq |z_{1/2}|$  and  $\rho^{\infty}(\mathbf{r}) = \sigma^{\infty} \delta(z)e^{ikx}$ , with  $\sigma^{\infty}$  being the asymptotic surface charge density. By integrating the continuity equation crossing the interface and exploiting the asymptotic equality between  $\mathbf{K}^{\infty}$  and  $\mathbf{K}_{\text{ind}}$ , we obtain the second boundary condition

$$\varepsilon_d(1 - r^{\text{nr}}) + (\varepsilon_d - 1)kd_{\parallel}(1 + r^{\text{nr}}) = [\varepsilon_m(1 + kd_{\parallel}) - kd_{\parallel}]t^{\text{nr}}, \quad (\text{S6})$$

where

$$d_{\parallel} = \frac{\int_{z_1}^{z_2} [K_{\text{ind}}^x(z) - K_x^{\infty}(z)] dz}{K_x^{\infty}(0^-) - K_x^{\infty}(0^+)}, \quad (\text{S7})$$

is the Feibelman parallel  $d$ -parameter. In the small wave vector limit, i.e.  $k \ll |z_{1/2}|^{-1}$ , the asymptotic current  $K_x^{\infty}(z)$  changes slowly over the region  $z \in [z_1, z_2]$ . This

\* anjhong@lzu.edu.cn

allows the following reduction

$$\begin{aligned}
d_{\parallel} &\simeq \frac{\int_{z_1}^{z_2} K_{\text{ind}}^x(z) dz + z_1 K_x^{\infty}(z_1) - z_2 K_x^{\infty}(z_2)}{K_x^{\infty}(z_1) - K_x^{\infty}(z_2)} \\
&= \frac{\int_{z_1}^{z_2} K_{\text{ind}}^x(z) dz + z_1 K_{\text{ind}}^x(z_1) - z_2 K_{\text{ind}}^x(z_2)}{K_{\text{ind}}^x(z_1) - K_{\text{ind}}^x(z_2)} \\
&= \frac{\int_{z_1}^{z_2} K_{\text{ind}}^x(z) dz - \int_{z_1}^{z_2} \partial_z [z K_{\text{ind}}^x(z)] dz}{-\int_{z_1}^{z_2} \partial_z K_{\text{ind}}^x(z) dz} \\
&= \frac{\int_{z_1}^{z_2} z \partial_z K_{\text{ind}}^x(z) dz}{\int_{z_1}^{z_2} \partial_z K_{\text{ind}}^x(z) dz}. \tag{S8}
\end{aligned}$$

Furthermore, because the field is localized in the region near the interface, one can safely extend the integration domain in Eq. (S8) to infinity. Solving the effective boundary conditions in Eqs. (S5) and (S6), the modified scattering coefficients can be obtained.

## II. SCATTERING COEFFICIENTS

The Feilbelman  $d$ -parameters can be interpreted in terms of effective boundary quantities at the interface. For instance, the  $d_{\perp}$ -parameter can be expressed in terms of a surface dipole density, while the  $d_{\parallel}$ -parameter can be incorporated as a current density. These surface quantities are [2, 3]

$$\boldsymbol{\pi} = -\varepsilon_0 d_{\perp} [[\nabla_{\perp} \phi]] \hat{\mathbf{n}}, \tag{S9}$$

$$\mathbf{K} = -i\varepsilon_0 \omega d_{\parallel} [[\varepsilon \nabla_{\parallel} \phi]]. \tag{S10}$$

Here,  $[[\cdot]]$  represents the discontinuities, i.e.

$$[[\nabla_{\perp} \phi]] = \nabla_{\perp} \phi(\mathbf{r}_{\parallel}^+) - \nabla_{\perp} \phi(\mathbf{r}_{\parallel}^-), \tag{S11}$$

$$[[\varepsilon \nabla_{\parallel} \phi]] = \varepsilon^+ \nabla_{\parallel} \phi(\mathbf{r}_{\parallel}^+) - \varepsilon^- \nabla_{\parallel} \phi(\mathbf{r}_{\parallel}^-), \tag{S12}$$

where the bulk permittivities  $\varepsilon^+ \equiv \varepsilon_d$  outside (i.e. at  $\mathbf{r}_{\parallel}^+ = \mathbf{r}_{\parallel} + 0^+ \hat{\mathbf{n}}$ ) and  $\varepsilon^- \equiv \varepsilon_m$  inside (i.e. at  $\mathbf{r}_{\parallel}^- = \mathbf{r}_{\parallel} - 0^+ \hat{\mathbf{n}}$ ) the interface extended along  $\mathbf{r}_{\parallel} = (x, y)$ , and  $\hat{\mathbf{n}}$  denotes the outward vector normal to the interface. These quantities can be easily generalized to the retarded regime. According to  $-\nabla \phi \rightarrow \mathbf{E}$  and  $-\varepsilon_0 \varepsilon \nabla \phi \rightarrow \mathbf{D}$ , we have [3, 4]

$$\boldsymbol{\pi} \equiv \varepsilon_0 d_{\perp} [[E_{\perp}]] \hat{\mathbf{n}} = \varepsilon_0 d_{\perp} [\hat{\mathbf{n}} \cdot (\mathbf{E}_d - \mathbf{E}_m)] \hat{\mathbf{n}}, \tag{S13}$$

$$\mathbf{K} \equiv i\omega d_{\parallel} [[\mathbf{D}_{\parallel}]] = i\omega d_{\parallel} [\hat{\mathbf{n}} \times (\mathbf{D}_d - \mathbf{D}_m) \times \hat{\mathbf{n}}]. \tag{S14}$$

Incorporating these surface densities in the macroscopic Maxwell boundary conditions  $[[\mathbf{E}_{\parallel}]] = -\varepsilon_0^{-1} \nabla_{\parallel} \boldsymbol{\pi}$  and  $[[\mathbf{H}_{\parallel}]] = \mathbf{K} \times \hat{\mathbf{n}}$  [5], we obtain the modified boundary conditions as

$$[[\mathbf{E}_{\parallel}]] = -d_{\perp} \nabla_{\parallel} [[E_{\perp}]], \tag{S15}$$

$$[[\mathbf{H}_{\parallel}]] = i\omega d_{\parallel} [[\mathbf{D}_{\parallel}]] \times \hat{\mathbf{n}}. \tag{S16}$$

Their explicit forms are

$$\mathbf{E}_{d\parallel} - \mathbf{E}_{m\parallel} = -d_{\perp} \nabla_{\parallel} [E_{d\perp} - E_{m\perp}], \tag{S17}$$

$$\mathbf{H}_{d\parallel} - \mathbf{H}_{m\parallel} = i\omega d_{\parallel} [\hat{\mathbf{n}} \times (\mathbf{D}_d - \mathbf{D}_m) \times \hat{\mathbf{n}}]. \tag{S18}$$

They indicate that the quantum surface effects make the parallel components of the electric and magnetic fields discontinuous, which is quite different from the ones in classical theory [6].

When the separation between the quantum emitter and the interface is small, the transverse magnetic (TM) waves contribution dominates the plasmon-enhanced light-matter interactions. Hence, we seek the scattering coefficients of the TM waves with a  $p$  polarization. Their wave functions are

$$\mathbf{H} = \begin{cases} (e^{-k_z d} z + r^p e^{i k_z d} z) e^{i(k_s x - \omega t)} \hat{\mathbf{y}}, & z > 0 \\ t^p e^{-i k_z m} z e^{i(k_s x - \omega t)} \hat{\mathbf{y}}, & z < 0 \end{cases}, \tag{S19}$$

$$\mathbf{E} = \begin{cases} [E_{x_d}(z) \hat{\mathbf{x}} + E_{z_d}(z) \hat{\mathbf{z}}] e^{i(k_s x - \omega t)}, & z > 0 \\ [E_{x_m}(z) \hat{\mathbf{x}} + E_{z_m}(z) \hat{\mathbf{z}}] e^{i(k_s x - \omega t)}, & z < 0 \end{cases} \tag{S20}$$

where  $r^p$  and  $t^p$  are the modified reflection and transmission coefficients,  $k_s$  and  $k_{z_d/m}$  are the wave-vector components parallel and perpendicular to the interface, satisfying  $k_s^2 + k_{z_d/m}^2 = \varepsilon_{d/m} \omega^2 / c^2$ . Substituting Eqs. (S19) and (S20) into Eqs. (S17) and (S18), we obtain

$$\frac{k_{z_d} (r^p - 1)}{\varepsilon_d} + \frac{k_{z_m} t^p}{\varepsilon_m} = i k_s^2 d_{\perp} \left( \frac{1 + r^p}{\varepsilon_d} - \frac{t^p}{\varepsilon_m} \right), \tag{S21}$$

$$d_{\parallel} [k_{z_d} (r^p - 1) + k_{z_m} t^p] = i(1 + r^p - t^p). \tag{S22}$$

Solving them and only retaining the linear-order terms of  $k_s d_{\perp, \parallel}$ , we obtain the scattering coefficients

$$\begin{aligned}
r^p &= \frac{\varepsilon_m k_{z_d} - \varepsilon_d k_{z_m} + i(\varepsilon_m - \varepsilon_d)(k_s^2 d_{\perp} - k_{z_d} k_{z_m} d_{\parallel})}{\varepsilon_m k_{z_d} + \varepsilon_d k_{z_m} - i(\varepsilon_m - \varepsilon_d)(k_s^2 d_{\perp} + k_{z_d} k_{z_m} d_{\parallel})}, \\
t^p &= \frac{2\varepsilon_d k_{z_m}}{\varepsilon_m k_{z_d} + \varepsilon_d k_{z_m} - i(\varepsilon_m - \varepsilon_d)(k_s^2 d_{\perp} + k_{z_d} k_{z_m} d_{\parallel})}.
\end{aligned}$$

In the classical limit,  $d_{\perp/\parallel} \rightarrow 0$  and thus Eqs. (S23) and (S23) retune to the traditional results in classical macroscopic electrodynamics [6].

## III. GREEN'S TENSOR OF THE METAL-DIELECTRIC INTERFACE

Given a layered structure composed by a metal in the regime of  $z < 0$  and a dielectric in the regime  $z > 0$  and a source point positioned above the interface, the Green's tensor is given by [5]

$$\mathbf{G}(\mathbf{r}, \mathbf{r}', \omega) = \begin{cases} \mathbf{G}_0(\mathbf{r}, \mathbf{r}', \omega) + \mathbf{G}_R(\mathbf{r}, \mathbf{r}', \omega), & z > 0 \\ \mathbf{G}_T(\mathbf{r}, \mathbf{r}', \omega), & z < 0 \end{cases}$$

where  $\mathbf{G}_0(\mathbf{r}, \mathbf{r}', \omega)$ ,  $\mathbf{G}_R(\mathbf{r}, \mathbf{r}', \omega)$  and  $\mathbf{G}_T(\mathbf{r}, \mathbf{r}', \omega)$  are the Green's tensors contributed by the free space, the reflected, and the transmitted field, respectively. Their explicit forms in Cartesian coordinate system are

$$\mathbf{G}_0(\mathbf{r}, \mathbf{r}', \omega) = \frac{i}{8\pi^2} \iint_{-\infty}^{\infty} \frac{1}{k_d^2 k_{zd}} \begin{bmatrix} k_d^2 - k_x^2 & -k_x k_y & \mp k_x k_{zd} \\ -k_x k_y & k_d^2 - k_y^2 & \mp k_y k_{zd} \\ \mp k_x k_{zd} & \mp k_y k_{zd} & k_d^2 - k_{zd}^2 \end{bmatrix} e^{ik_{zd}(z-z')} d\mathbf{k}_{\parallel}, \quad (\text{S23})$$

$$\mathbf{G}_R(\mathbf{r}, \mathbf{r}', \omega) = \frac{i}{8\pi^2} \iint_{-\infty}^{\infty} \frac{-r^P}{k_d^2 (k_x^2 + k_y^2)} \begin{bmatrix} k_x^2 k_{zd} & k_x k_y k_{zd} & k_x (k_x^2 + k_y^2) \\ k_x k_y k_{zd} & k_y^2 k_{zd} & k_y (k_x^2 + k_y^2) \\ -k_x (k_x^2 + k_y^2) & -k_y (k_x^2 + k_y^2) & -(k_x^2 + k_y^2)^2 / k_{zd} \end{bmatrix} e^{ik_{zd}(z+z')} d\mathbf{k}_{\parallel}, \quad (\text{S24})$$

$$\mathbf{G}_T(\mathbf{r}, \mathbf{r}', \omega) = \frac{i}{8\pi^2} \iint_{-\infty}^{\infty} \frac{t^P}{k_d k_m (k_x^2 + k_y^2)} \begin{bmatrix} k_x^2 k_{zm} & k_x k_y k_{zd} & k_x (k_x^2 + k_y^2) k_{zm} / k_{zd} \\ k_x k_y k_{zd} & k_y^2 k_{zd} & k_y (k_x^2 + k_y^2) k_{zm} / k_{zd} \\ k_x (k_x^2 + k_y^2) & k_y (k_x^2 + k_y^2) & (k_x^2 + k_y^2)^2 / k_{zd} \end{bmatrix} e^{i(k_{zd} z' - k_{zm} z)} d\mathbf{k}_{\parallel} \quad (\text{S25})$$

where  $d\mathbf{k}_{\parallel} = e^{i[k_x(x-x') + k_y(y-y')]} dk_x dk_y$ , the upper sign applies for  $z > z'$ , and the lower sign applies for  $z < z'$ .

Choosing the dipole moment perpendicular to the interface, i.e.,  $\boldsymbol{\mu}_i = \mu \mathbf{e}_z$ , only the  $zz$  component of the Green's tensor contributes to the QE-SPP interaction. It is written as

$$G_{zz}(\mathbf{r}, \mathbf{r}', \omega) = \frac{i}{8\pi^2} \iint_{-\infty}^{\infty} \frac{k_s^2}{k_d^2 k_{zd}} [e^{ik_{zd}(z-z')} + r^P e^{ik_{zd}(z+z')}] \times e^{i[k_x(x-x') + k_y(y-y')]} dk_x dk_y, \quad (\text{S26})$$

where  $k_s^2 = k_x^2 + k_y^2 = k_d^2 - k_{zd}^2$ . Substituting  $k_x = k_s \cos \varphi$ ,  $k_y = k_s \sin \varphi$ , and  $dk_x dk_y = k_s dk_s d\varphi$  and performing the integral over  $\varphi$ , we obtain

$$G_{zz}(\mathbf{r}, \mathbf{r}', \omega) = \int_0^{\infty} \frac{dk_s}{4\pi} \frac{i J_0(k_s r_{\parallel})}{k_d^2 k_{zd} k_s^{-3}} (e^{ik_{zd} z^-} + r^P e^{ik_{zd} z^+}), \quad (\text{S27})$$

where  $r_{\parallel} = \sqrt{(x-x')^2 + (y-y')^2}$ ,  $z^{\pm} = z \pm z'$ , and  $J_0(x)$  is the zeroth-order Bessel function of the first kind.

#### IV. ENERGY SPECTRUM

The eigenstate of the Hamiltonian of the total system formed by the quantum emitters and the surface plasmon polariton in the single-excitation subspace can be expanded as  $|\Phi\rangle = [\sum_{i=1}^N x_i \hat{\sigma}_i^{\dagger} + \int d^3\mathbf{r} \int d\omega y_{\mathbf{r},\omega} \hat{\mathbf{f}}^{\dagger}(\mathbf{r}, \omega)] |G; \{0_{\mathbf{r},\omega}\}\rangle$ . From the stationary Schrödinger equation  $\hat{H}|\Phi\rangle = E|\Phi\rangle$ , with  $E$  being the eigenenergy of the total system, we have

$$(\hbar\omega_0 - E)x_i = \int d\omega \int d^3\mathbf{r} \frac{i\omega^2 c^{-2}}{\sqrt{\pi\epsilon_0/\hbar}} \sqrt{\text{Im}[\epsilon_m(\omega)]} \times \boldsymbol{\mu}_i \cdot \mathbf{G}(\mathbf{r}_i, \mathbf{r}, \omega) y_{\mathbf{r},\omega}, \quad (\text{S28})$$

$$(E - \hbar\omega_0)y_{\mathbf{r},\omega} = \frac{i\omega^2 c^{-2}}{\sqrt{\pi\epsilon_0/\hbar}} \sqrt{\text{Im}[\epsilon_m(\omega)]} \times \sum_{i=0}^N \boldsymbol{\mu}_i^* \cdot \mathbf{G}^*(\mathbf{r}_i, \mathbf{r}, \omega) x_i. \quad (\text{S29})$$

Substituting the solution  $y_{\mathbf{r},\omega}$  of Eq. (S29) into Eq. (S28) and using  $\text{Im}[\mathbf{G}(\mathbf{r}_i, \mathbf{r}_j, \omega)] =$

$\int d^3\mathbf{r} \frac{\omega^2}{c^2} \text{Im}[\epsilon_m(\omega)] \mathbf{G}(\mathbf{r}_i, \mathbf{r}, \omega) \mathbf{G}^*(\mathbf{r}_j, \mathbf{r}, \omega)$  and the spectral density matrix defined in the main text, we obtain

$$[E - \hbar\omega_0 - \hbar^2 \int d\omega \frac{\mathbf{J}(\omega)}{E - \hbar\omega}] \mathbf{x} = 0, \quad (\text{S30})$$

where  $\mathbf{x} = (x_1, \dots, x_N)^T$ . Only when the determinant of the coefficient matrix is zero, Eq. (S30) has nontrivial solution. Then, we obtain the eigen-equations

$$\omega_0 - \int d\omega \frac{A_j(\omega)}{\omega - E/\hbar} = \frac{E}{\hbar}, \quad (\text{S31})$$

where we have used the Jordan decomposition of  $\mathbf{J}(\omega) = \mathbf{C}\mathbf{A}(\omega)\mathbf{C}^{-1}$ , with  $\mathbf{C}$  and  $\mathbf{A}(\omega) = \text{diag}[A_1(\omega), \dots, A_N(\omega)]$  being its similarity matrix and Jordan canonical form. Equation (S31) has a same form to Eq. (6) in the main text determining the dynamics. It reveals that energy-spectrum character of the total system plays a decisive role in the dynamics of quantum emitters.

#### V. STEADY-STATE SOLUTION

The long-time form of Eq. (7) is derived as follows.

When  $N = 1$ , the spectral density reads  $\mathbf{J}(\omega) = J_0(\omega)$ . Then, the Laplace transform of  $a(t)$  reduces to  $\tilde{a}(s) = [s + i\omega_0 + \int_0^{\infty} \frac{J_0(\omega)}{s + i\omega} d\omega]^{-1}$ . If a bound state with eigenenergy  $\hbar\omega^b$  is formed, then the residue contributed by it is

$$\mathbf{Z}(t) = \lim_{s \rightarrow -i\omega^b} \frac{(s + i\omega^b) e^{st}}{s + i\omega_0 + \int_0^{\infty} \frac{J_0(\omega)}{s + i\omega} d\omega} = L_0 e^{-i\omega^b t}, \quad (\text{S32})$$

where  $L_0 = [1 + \int d\omega \frac{J_0(\omega)}{(\omega - \omega^b)^2}]^{-1}$ .

When  $N = 2$ , the spectral density matrix is

$$\mathbf{J}(\omega) = \begin{pmatrix} J_0(\omega) & J_1(\omega) \\ J_1(\omega) & J_0(\omega) \end{pmatrix}. \quad (\text{S33})$$

and the initial condition is  $\mathbf{a}(0) = (1, 0)^T$ . The Laplace transform of  $\mathbf{a}(t)$  is

$$\tilde{\mathbf{a}}(s) = \begin{pmatrix} 1 & 1 \\ 1 & -1 \end{pmatrix} \begin{pmatrix} l_{01}^{(1)}(s) \\ l_{01}^{(2)}(s) \end{pmatrix}, \quad (\text{S34})$$

where  $l_{mn}^{(j)}(s) = [s + i\omega_0 + \int d\omega \frac{J_m(\omega) - (-1)^j J_n(\omega)}{s + i\omega}]^{-1}/2$ . The residue contributed by the  $l$ th bound state with frequency  $\varpi_l^b$  evaluated by  $Y_l(\varpi) = \varpi$  to the inverse Laplace transform of  $l_{01}^{(j)}(s)$  is

$$\lim_{s \rightarrow -i\varpi_l^b} (s + i\varpi_l^b) e^{st} l_{01}^{(j)}(s) = L_{01}^{(j)} e^{-i\varpi_l^b t} \delta_{l,j}, \quad (\text{S35})$$

where  $L_{01}^{(j)}(\varpi) = [\partial_s l_{01}^{(j)}|_{s=-i\varpi_j^b}]^{-1}$ . Therefore, if  $M$  bound states are formed, then we have

$$\mathbf{Z}(t) = \sum_{j=1}^M L_{01}^{(j)} \begin{pmatrix} 1 \\ (-1)^{j+1} \end{pmatrix} e^{-i\varpi_j^b t}. \quad (\text{S36})$$

- 
- [1] P. J. Feibelman, Surface electromagnetic fields, [Prog. Surf. Sci. \*\*12\*\*, 287 \(1982\)](#).
  - [2] T. Christensen, W. Yan, A.-P. Jauho, M. Soljačić, and N. A. Mortensen, Quantum corrections in nanoplasmonics: Shape, scale, and material, [Phys. Rev. Lett. \*\*118\*\*, 157402 \(2017\)](#).
  - [3] Y. Yang, D. Zhu, W. Yan, A. Agarwal, M. Zheng, J. D. Joannopoulos, P. Lalanne, T. Christensen, K. K. Berggren, and M. Soljačić, A general theoretical and experimental framework for nanoscale electromagnetism, [Nature \*\*576\*\*, 248 \(2019\)](#).
  - [4] P. A. D. Gonçalves, T. Christensen, N. Rivera, A.-P. Jauho, N. A. Mortensen, and M. Soljačić, Plasmon-emitter interactions at the nanoscale, [Nat. Commun. \*\*11\*\*, 366 \(2020\)](#).
  - [5] L. Novotny and B. Hecht, [Principles of Nano-optics](#) (Cambridge University Press, Cambridge, UK, 2012).
  - [6] C.-J. Yang and J.-H. An, Suppressed dissipation of a quantum emitter coupled to surface plasmon polaritons, [Phys. Rev. B \*\*95\*\*, 161408 \(2017\)](#).